Approach to the Atmospheric Chemistry of Methyl Nitrate and Methylperoxy Nitrite. Chemical Mechanisms of Their Formation and Decomposition Reactions in the Gas Phase

Juan F. Arenas, Francisco J. Avila, Juan C. Otero, Daniel Peláez, and Juan Soto*

University of Málaga, Physical Chemistry, Faculty of Science, Málaga, 29071, Spain

Received: July 16, 2007; In Final Form: September 19, 2007

Potential energy surfaces, minimum energy reaction paths, minima, transition states, reaction barriers, and conical intersections for the most important atmospheric reactions of methyl nitrate (CH_3ONO_2) and methylperoxy nitrite (CH_3OONO) on the electronic ground state have been studied (i) with the second-order multiconfigurational perturbation theory (CASPT2) by computation of numerical energy gradients for stationary points and (ii) with the density functional theory (DFT). The proposed mechanism explains the conversion of unreactive alkyl peroxy radicals into alkoxy radicals: $CH_3O_2 + NO \leftrightarrows CH_3OONO \leftrightarrows CH_3O + NO_2 \leftrightarrows CH_3ONO_2$. Additionally, several discrepancies found in the comparison of the results obtained from the two employed approaches are analyzed. CASPT2 predicts that all dissociation reactions into radicals occur without an extra exit energy barrier. In contrast, DFT finds transition states for the dissociations of *cis*- and *trans*-methylperoxy nitrite into $CH_3O + NO_2$. Furthermore, multiconfigurational methods [CASPT2 and complete active space SCF (CAS-SCF)] predict the isomerization of CH_3ONO_2 to CH_3OONO to occur in a two-step mechanism: (i) $CH_3ONO_2 \rightarrow CH_3O + NO_2$; and (ii) $CH_3O + NO_2 \rightarrow CH_3OONO$. The reason for this has to do with the coupling of the ground electronic state with the first excited state. Therefore, it is demonstrated that DFT methods based on single determinantal wave functions give an incorrect picture of the aforementioned reaction mechanisms.

Introduction

Alkyl nitrates ($RONO_2$) and alkyl peroxynitrites (ROONO) are important molecules in the chemistry of the atmosphere. These two species have both anthropogenic and biogenic origins,[1−3] for example, it has been recently discovered that an important amount of tropospheric methyl nitrate arises from an unknown marine source.[1−3] Alkyl nitrate and alkyl peroxynitrites are related to each other through the chemistry of organic peroxy radicals (ROO•). Such radicals, which are formed in the oxidation of anthropogenic or biogenic volatile organic compounds, combine with nitric oxide (NO) to produce alkoxy radicals (RO•) and nitrogen dioxide (NO_2) plus a significant amount of alkyl nitrates.[3]

$$ROO\bullet + NO \rightarrow RO\bullet + NO_2 \quad (1)$$

$$\rightarrow RONO_2 \quad (2)$$

It is accepted that the mechanisms of both reactions share a common intermediate, peroxynitrite, (Scheme 1).[3−11] Recent theoretical works[8−10] have characterized a transition state for the ROONO → $RONO_2$ isomerization reaction by using density functional theory (DFT). Negative temperature dependence of the rate coefficients for reactions 1 and 2 also suggests that ROONO is an intermediate.[11] However, the ROONO intermediate itself has not been observed in the gas phase for R≠H.[6] Reaction 1 is important because it converts relatively unreactive alkyl peroxy radicals and nitric oxide to highly reactive alkoxy radicals and NO_2. In turn, photolysis of NO_2 is the only known way of producing ozone in the troposphere via reactions 3 and 4.[12] Furthermore, since reaction 2 competes with ozone formation, it limits the production of O_3 whose presence in the troposphere causes crop damage and human respiratory illness.[4]

SCHEME 1: Accepted Mechanism for Reaction of Alkyl Peroxy Radicals with Nitric Oxide

$$NO_2 + h\nu \rightarrow O + NO \quad (3)$$

$$O + O_2 + M \rightarrow O_3 + M \quad (4)$$

The main objective of the present work is to study the chemistry of methyl nitrate and methylperoxy nitrite on their electronic ground states. This paper is structured in four sections: (i) Introduction, in which the most relevant preceding works are summarized; (ii) Computational Details, where the methods of calculation are described; (iii) Results and Discussion, which deals with dissociation reactions of methyl nitrate and methylperoxy nitrite, rearrangement of methyl nitrate to methylperoxy nitrite, and formaldehyde elimination from methyl nitrate and methylperoxy nitrite, respectively; and (iv) Conclusions.

It is noteworthy that the decomposition channel of methyl nitrate into CH_3 and NO_3 has not been studied in this work. However, the bond dissociation energy computed from tabulated experimental data amounts to 81.8 kcal/mol (Table 1), a value which is rather high to be considered as a competitive channel.

* Corresponding author. Fax: +34-952132047. E-mail: soto@uma.ps.

10.1021/jp075546n CCC: $40.75
Published on Web 12/18/2007

TABLE 1: Energetic of Dissociation Reactions of CH_3ONO_2 and CH_3OONO (CASPT2//CAS-SCF(16e,12o))[a]

reaction	ΔE[b]	$\Delta U(0)$[c]	ΔH[d]	exptl[e]
$CH_3ONO_2 \rightarrow CH_3 + NO_3$				81.8 (342.1)
$CH_3ONO_2 \rightarrow CH_3O + NO_2$	47.5	42.2 (176.7)[f]	43.4 (181.5)	41.2 (172.4)
$CH_3ONO_2 \rightarrow$ Ci1	38.0			
$CH_3ONO_2 \rightarrow$ Ci2	84.7			
$CH_3ONO_2 \rightarrow H_2CO + HONO$	42.0	36.6 (153.2)	36.8 (153.9)	
c-$CH_3OONO \rightarrow CH_3O + NO_2$	15.1	11.8 (49.3)	12.5 (52.1)	
c-$CH_3OONO \rightarrow CH_3OO + NO$	26.4	25.2 (105.4)	26.4 (110.4)	
t-$CH_3OONO \rightarrow CH_3O + NO_2$	13.2	9.9 (41.5)	10.5 (44.0)	
t-$CH_3OONO \rightarrow CH_3OO + NO$	24.3	23.2 (97.1)	24.3 (101.9)	
		36.6 (153.2)	36.8 (153.9)	

[a] Four state average reference wave function. [b] Difference in electronic energies in kcal mol^{-1}. [c] Difference in electronic energies plus zero-point energies in kcal mol^{-1}. [d] Dissociation enthalpy at $T = 298.15$ K. [e] Bond dissociation energy calculated as $D° = \sum \Delta_f H°(\text{product}) - \Delta_f H°(\text{reactant})$ from *CRC Handbook of Chemistry and Physics* 2002−2003, 83rd ed.; Lide, D. R., Ed.; CRC Press LLC: Boca Raton, FL, 2002. [f] Values in parentheses in kJ/mol.

Computational Details

All of the geometry optimizations of the relevant species involved in the reactions of methyl nitrate and methylperoxy nitrite have been performed in Cartesian coordinates and using generally contracted basis sets of the atomic natural orbital (ANO) type obtained from the C,N,O(14*s*9*p*4*d*3*f*)/H(8*s*4*p*3*d*) primitive sets,[13] the so-called ANO-L basis sets, with the C,N,O-[4*s*3*p*2*d*1*f*]/H[3*s*2*p*1*d*] contraction schemes. These optimizations were performed following two strategies: (i) optimization at the complete active space self-consistent field (CAS-SCF)[14] level of theory by computation of analytical energy gradients, and (ii) optimizations with the second-order multiconfigurational perturbation theory (CASPT2)[15] by computation of numerical energy gradients. Both methods were applied as implemented in the MOLCAS 6.2 program.[16] In the CASPT2 calculations, the 1*s* electrons of the carbon, oxygen, and nitrogen atoms, as determined in the SCF calculations were kept frozen. The stationary points (minima and saddle points) were characterized by their CASSCF analytic harmonic vibrational frequencies computed by diagonalizing the mass-weighted Cartesian force constant matrix. On the other hand, the localization of the crossing points was done with the algorithm[17] implemented in the GAUSSIAN program[18] and with the cc-pVDZ basis sets.[19] The gradient difference and non-adiabatic coupling vectors were computed by using state average orbitals in the manner suggested by Yarkony.[20]

Selection of the active space is crucial in the CAS-SCF calculations of methyl nitrate and methylperoxy nitrite. To avoid undesirable effects on the wave function such as symmetry breaking, the minimum active space must comprise 14 electrons distributed in 11 orbitals, in accordance with reported works[21] on related nitro-derivatives. These orbitals correspond to the 2*s*-orbital of nitrogen atom, two NO bonding orbitals σ_{NO}, one delocalized ONO π-bonding orbital π_{NO}, one σ-nonbonding orbital nσ_O, one π-nonbonding orbital nπ_O, two NO antibonding orbitals σ^*_{NO}, one delocalized ONO π-antibonding orbital π^*_{NO}, plus CN bonding and antibonding orbitals σ_{CN} and σ^*_{CN} on CH_3ONO_2. Moreover, the active space has been increased in some calculations by adding the nonbonding np_O orbital of the methoxy group, which results in a 16 electron 12 orbital active space. Along the text, the active space used in each case will be specified.

The topology of the potential energy surfaces has been studied performing linear interpolations and reduced two-dimensional potential energy surfaces. Linear interpolations for dissociations of CH_3ONO_2 and CH_3OONO into radicals are built in the following manner: electronic energies are represented versus an interpolation vector, $\Delta\boldsymbol{R}$, which connects ground state minima of stable molecules with their respective ground-state dissociation products. This vector is built by calculating the difference between internal coordinates of reactant and dissociation products, $\Delta\boldsymbol{R} = \boldsymbol{R}_i - \boldsymbol{R}_j$, where $\boldsymbol{R}_i$ and $\boldsymbol{R}_j$ represent the internal coordinate vectors of the initial and dissociation products, respectively.[21]

Reduced two-dimensional surfaces are built from sets of perfectly ordered points.[22] Two orthogonal directions are obtained as follows:

(i) Two generator vectors are defined in internal coordinates as

$$\boldsymbol{R}_1 = \boldsymbol{R}(\mathrm{I}) - \boldsymbol{R}(\mathrm{J}) \tag{5a}$$

$$\boldsymbol{R}_2 = \boldsymbol{R}(\mathrm{I}) - \boldsymbol{R}(\mathrm{K}) \tag{5b}$$

where $\boldsymbol{R}$(L) denotes the internal coordinate vector of a given species.

(ii) Vectors $\boldsymbol{R}_1$ and $\boldsymbol{R}_2$ are normalized

$$\boldsymbol{r}_1 = \frac{\boldsymbol{R}_1}{\boldsymbol{R}_1} \tag{6}$$

$$\boldsymbol{r}_2 = \frac{\boldsymbol{R}_2}{\boldsymbol{R}_2} \tag{7}$$

(iii) Sum and subtraction of $\boldsymbol{r}_1$ and $\boldsymbol{r}_2$ give a set of two orthogonal vectors,

$$\boldsymbol{r}_a = \boldsymbol{r}_1 + \boldsymbol{r}_2 \tag{8}$$

$$\boldsymbol{r}_b = \boldsymbol{r}_1 - \boldsymbol{r}_2 \tag{9}$$

(iv) Vectors $\boldsymbol{r}_a$ and $\boldsymbol{r}_b$ are scaled by the length of the largest vector between $\boldsymbol{R}_1$ and $\boldsymbol{R}_2$.

$$\boldsymbol{R}_a = \boldsymbol{R}_2 \cdot \boldsymbol{r}_a \tag{10}$$

$$\boldsymbol{R}_b = \boldsymbol{R}_2 \cdot \boldsymbol{r}_b \tag{11}$$

To finish this section, it must be remarked that density functional theory (DFT) with the B3-LYP[23] nonlocal exchange correlation functional has been applied as well to study the title molecules. For each transition state localized at this level of theory, intrinsic reaction coordinate[24] (IRC) calculations have been performed as well. Thus, the products and reagents

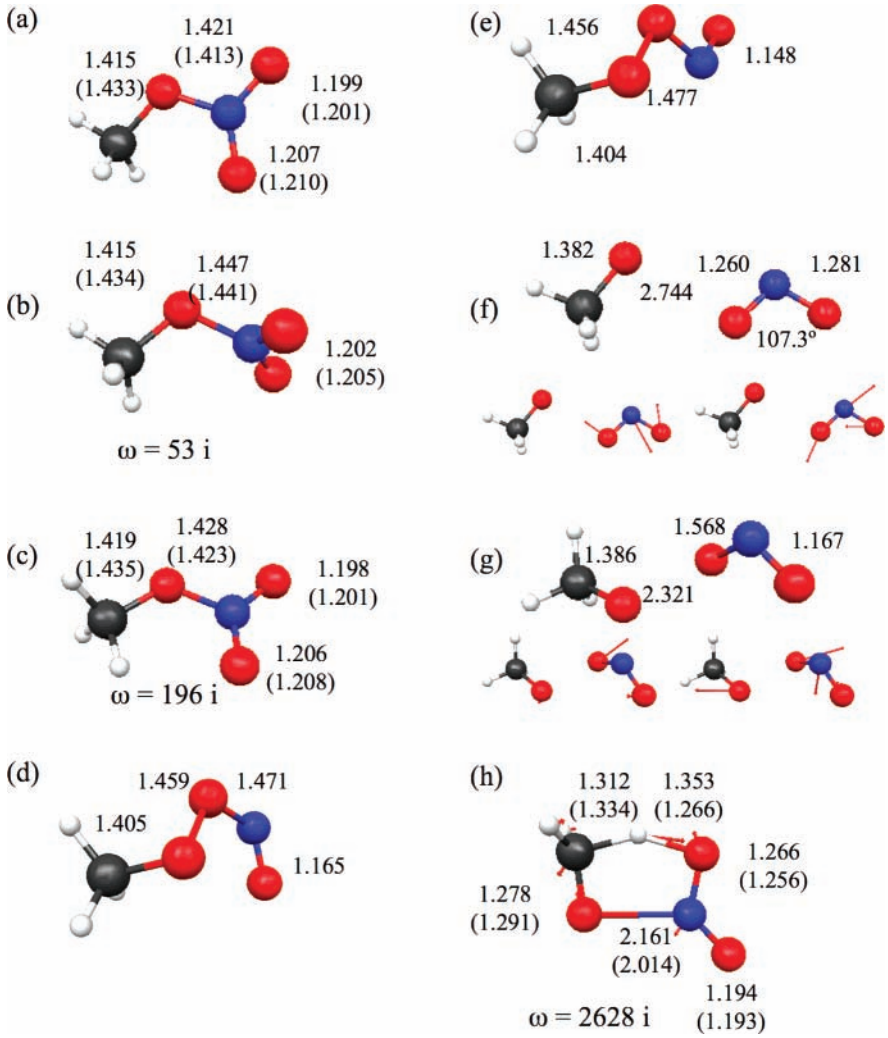

Figure 1. CAS-SCF geometries (in parentheses selected CASPT2 parameters) of the relevant species for the decomposition and isomerization of methyl nitrate: (a) staggered methyl nitrate (M1); (b) saddle point for $-NO_2$ rotation (Sd1); (c) saddle point for $-CH_3$ rotation (Sd2); (d) *cis*-methylperoxy nitrite (M2); (e) *trans*-methylperoxy nitrite (M3); (f) S_1/S_0 conical intersection (Ci1), the arrows in the smaller figures correspond to nonadiabatic coupling (left) and gradient difference (right) vectors; (g) S_1/S_0 conical intersection (Ci2); (h) transition state for nitrous acid elimination from methyl nitrate (Ts1). Imaginary frequencies computed analytically at the CAS-SCF level.

connected by the respective transition states have been unambiguously localized.

Results and Discussion

This section is organized as follows. Prior to discussion of the reaction mechanisms, all of the critical points found in this study are illustrated in Figure 1 and have been plotted with the MacMolplt program.[25] Second, it is shown that the dissociation reactions of the three stable species dealt with in this work, namely, CH_3ONO_2, *cis*-CH_3OONO, and *trans*-CH_3OONO, occur without any extra exit energy barrier. Therefore, the association reactions of the corresponding radicals are barrierless. Third, the nitro−nitrite isomerization of methyl nitrate ($CH_3ONO_2 \rightarrow CH_3OONO$) is discussed. Fourth, we study elimination reactions of the three cited species to yield HCHO and HONO (or HNO_2). To finish, the bimolecular reaction $2CH_3ONO_2 \rightarrow CH_3ONO + HOCH_2ONO_2$ is analyzed.

The microwave spectrum of CH_3ONO_2 yields a planar heavy-atom skeleton with the methyl group staggered with respect to the cis oxygen atom.[26,27] Rough relative intensity measurements of the bands of the microwave spectrum yield a barrier of 9.1 ± 2.6 kcal/mol for NO_2 internal rotation and 2.3 kcal/mol for internal rotation of the methyl group.[26] Figure 1a displays the optimized geometry of the staggered minimum of CH_3ONO_2 at the CASSCF and CASPT2 levels. Figure 1, parts b and c, represent two stationary structures of CH_3ONO_2 that correspond to saddle points for rotation of the NO_2 and CH_3 moieties, respectively. The computed barriers for these two internal rotations agree well with the experimental data reported above; they amount to 6.1 and 2.3 kcal/mol, respectively. Concerning methylperoxy nitrite, two conformers have been located, *cis*- and *trans*-methylperoxy nitrite (Figure 1, parts d and e). Figure 1, parts f and g, represent two S_1/S_0 conical intersections, which are relevant in the dissociation and isomerization mechanisms of *trans*-methylperoxy nitrite and methyl nitrate, alternately. Finally, Figure 1h represents the transition state (Ts1) leading to the decomposition of methyl nitrate into formaldehyde and nitrous acid. Internal coordinates of all these points are collected in the Supporting Information section, Table S1.

Dissociation Reactions of Methyl Nitrate and Methylperoxy Nitrite. The most striking result obtained in this section is that decompositions of the title molecules into radicals (RO• + NO_2 or ROO• + NO) take place without an extra exit barrier; in other words, the reverse reactions of the free radicals to yield the closed-shell reactants are barrierless. This is in contrast with the conclusions which can be extracted from B3-LYP calcula-

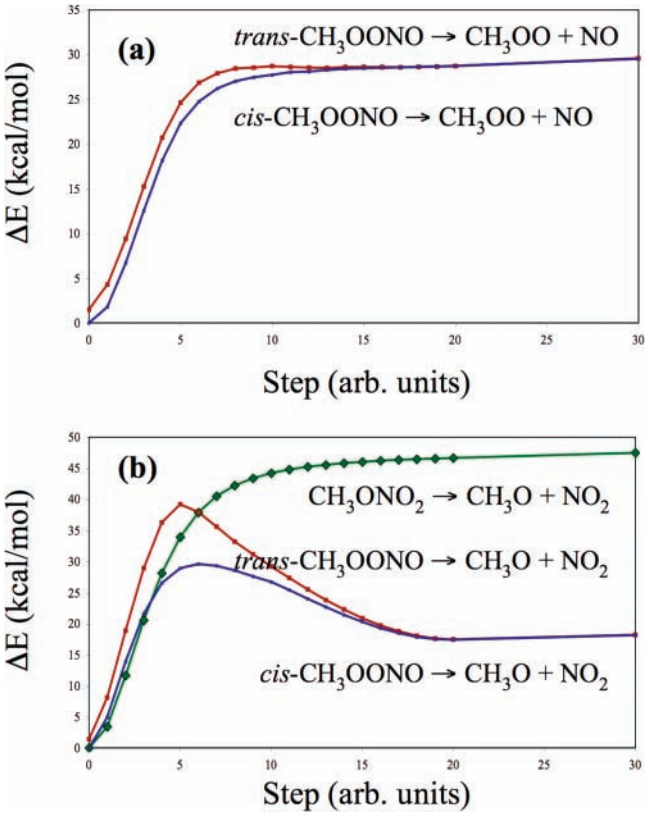

Figure 2. MS-CASPT2 energy profiles of the dissociation reactions (a) $CH_3OONO \rightarrow CH_3OO + NO$, and (b) $R(O)NO_2 \rightarrow R(O) + NO_2$.

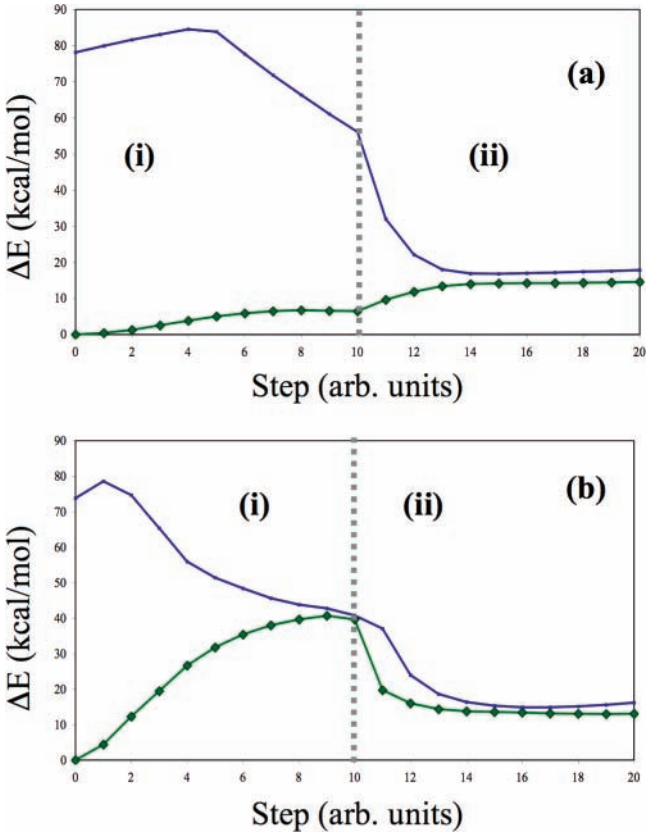

Figure 3. MS-CASPT2 energies profiles for dissociations of *cis*- and *trans*-methylperoxy nitrite into CH_3O and NO_2. (a) Linear interpolations (i) from *cis*-methylperoxy nitrite to Ts2, and (ii) from Ts2 to $CH_3O + NO_2$. (b) Linear interpolations (i) from *trans*-methylperoxy nitrite to Ts3, and (ii) from Ts3 to $CH_3O + NO_2$.

tions as it will be illustrated in the next paragraphs. The energetic of the dissociation reactions which will be discussed in this manuscript is presented in Table 1.

Figure 2a shows the linear interpolations for the dissociation of *cis*- and *trans*-methylperoxy nitrite into CH_3OO and NO. It is clearly observed here that elimination of nitric oxide occurs without an extra exit barrier. Consequently, we must conclude that there is no saddle point on the *3N*-dimensional potential energy hypersurface for such a process in both conformers. Alternatively, Figure 2b plots the energy profile for NO_2 production from methyl nitrate and methylperoxy nitrite. The dissociative interpolation of CH_3ONO_2 yields no extra exit barrier for NO_2 formation; therefore, again, there is no saddle point on the potential energy surface for this reaction. On the other hand, interpolations for dissociations of both conformers of methylperoxy nitrite yield a remarkable exit barrier. These maxima on the one-dimensional potential energy curves might suggest that transition states for such reactions could exist. In fact, we were able to find them at the (U)B3-LYP level (Ts2 and Ts3, respectively). The spin contamination was moreover significant ($S^2 = 0.4$) for both structures. Their geometries and relative energies are in perfect agreement with the previously published data.[10,28] The geometrical parameters, energetic of the reactions, and energy profiles of the intrinsic reaction coordinates for the dissociation through the respective transition states of *cis*- and *trans*-methylperoxy nitrite are included in the Supporting Information section (Table S2 and S3, and Figure S1). In contrast, any attempt to characterize these two transitions states at the CASPT2 level yielded no results. The reason for this is that both transition states do not exist at all. We base this statement on the energy profiles represented in Figure 3. Figure 3a shows the MS-CASPT2 linear interpolations (i) from *cis*-methylperoxy nitrite to Ts2 (B3-LYP) and (ii) from Ts2 to $CH_3O + NO_2$. It is clearly observed in Figure 3a that dissociation products ($CH_3O + NO_2$) are reached without surmounting any extra energy barrier; therefore, by definition, no transition state exists for dissociation of the cis conformer on the potential energy surface. The structure corresponding to the transition state localized by the B3-LYP method is simply a wiggle on the potential surface. Concerning the dissociation of *trans*-methylperoxy nitrite, we must conclude again that the saddle point (Ts3) characterized by the B3-LYP method is an artifact. When the calculations are performed at the most sophisticated MS-CASPT2 level, the structure of Ts3 corresponds to a surface crossing as shown in Figure 3b; in fact, we were able to localize the minimum energy point in such a conical intersection with the CAS-SCF method (Ci1, Figure 1f). Furthermore, the origin of this crossing is closely related to the C_{2v} conical intersection between the $^2A_1/^2B_2$ states of NO_2.[29] The search of this conical intersection of NO_2 at the CAS-SCF (13, 10) with the cc-pvDZ basis sets yields an internuclear distance $R(NO) = 1.271$ Å and an angle $\theta(ONO) = 107.2°$. Both geometrical parameters of the $^2A_1/^2B_2$ conical intersection are close to those found in the $-NO_2$ fragment of Ci1 (Figure 1f).

Rearrangement of Methyl Nitrate to Methylperoxy Nitrite. We were able to find with the B3-LYP method a transition state (Ts4) for the nitro−nitrite rearrangement of methyl nitrate. The geometrical parameters and intrinsic reaction coordinate are given in the Supporting Information section, Table S4 and Figure S2, respectively. The energetic of the reaction was given in Table S3. The IRC calculation clearly demonstrates that this structure (Ts4) is the transition state for the isomerization of methyl nitrate to *cis*-methylperoxy nitrite at this level of theory. However, when the search was tried with the CAS-SCF approximation, it was impossible to localize this transition state.

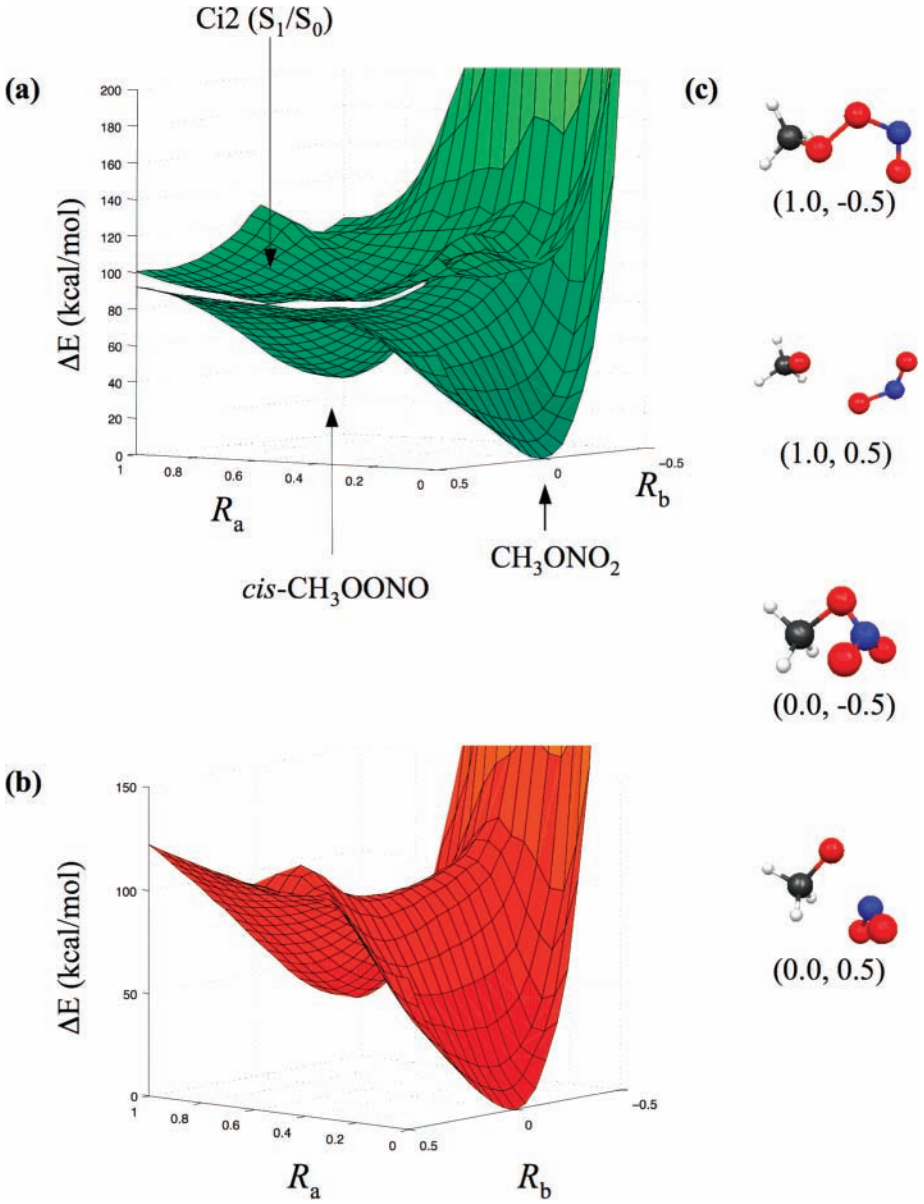

Figure 4. Potential energy surfaces for $CH_3ONO_2 \rightarrow$ *cis*-CH_3OONO reaction (a) S_0 and S_1 surfaces at the CASPT2 level with CAS (14, 11) reference active space, (b) S_0 B3-LYP/aug-cc-pvdz surface showing a saddle point between CH_3ONO_2 and *cis*-CH_3OONO, and (c) molecular arrangements of the four corners of the surfaces, labels denote coordinates. $\boldsymbol{R}$(I) = $\boldsymbol{R}$(CH_3ONO_2); $\boldsymbol{R}$(J) = $\boldsymbol{R}$(*cis*-CH_3OONO); $\boldsymbol{R}$(K) = $\boldsymbol{R}$(Ci2).

The only critical point that we found in the neighborhood of Ts4 was an S_1/S_0 conical intersection (Ci2, Figure 1g). This is exactly the same finding that was observed in the nitro−nitrite isomerization of nitramide.[22] Therefore, we have followed the methodology that was applied to nitramide. That is, to clarify the discrepancy found between multiconfigurational and Hartree−Fock-based methods, the reduced two-dimensional potential energy surfaces for the isomerization reaction of methyl nitrate have been built at the state-averaged CAS-SCF level of theory including both the S_0 and S_1 states with the MS-CASPT2 approach (Figure 4a). The points which generate these surfaces expand the geometries of four critical molecular arrangements: (i) methyl nitrate (M1), the (ii) S_1/S_0 conical intersection (Ci2), (iii) *cis*-CH_3OONO (M2), and (iv) dissociation products (CH_3O + NO_2). The most striking feature of this figure is the S_1/S_0 conical intersection. Additionally, a reaction path leading to dissociation of methyl nitrate into CH_3O + NO_2 on the S_0 surface is observed, but no transition state appears for the direct isomerization. The reason for this behavior can be attributed to the presence of such a conical intersection, which destroys the S_0 transition state for isomerization.

Figure 4b shows the B3-LYP/aug-cc-pVDZ potential energy surface of the nitro−nitrite isomerization of methyl nitrate, which has been built with the same geometrical points used in Figure 4a. Although the geometry of the transition state has not been specifically included, the reaction path for direct isomerization passing through a saddle point is observed in such a figure. This fact strengthens our confidence in that the reduced dimensionality energy surfaces are representative of the reaction mechanisms. That is, if the transition state for isomerization would exist at the CAS-SCF level, we had been indeed able to find it. There are several reasons to think that the picture given for the isomerization process by the DFT methods based on monoconfigurational wavefunctions are not but artifacts. First, the weight of the Hartree−Fock configuration on the multiconfigurational wavefunction amounts only to ~60% around the region of the conical intersection, just where restricted approaches localize the transition state. Second, these methods

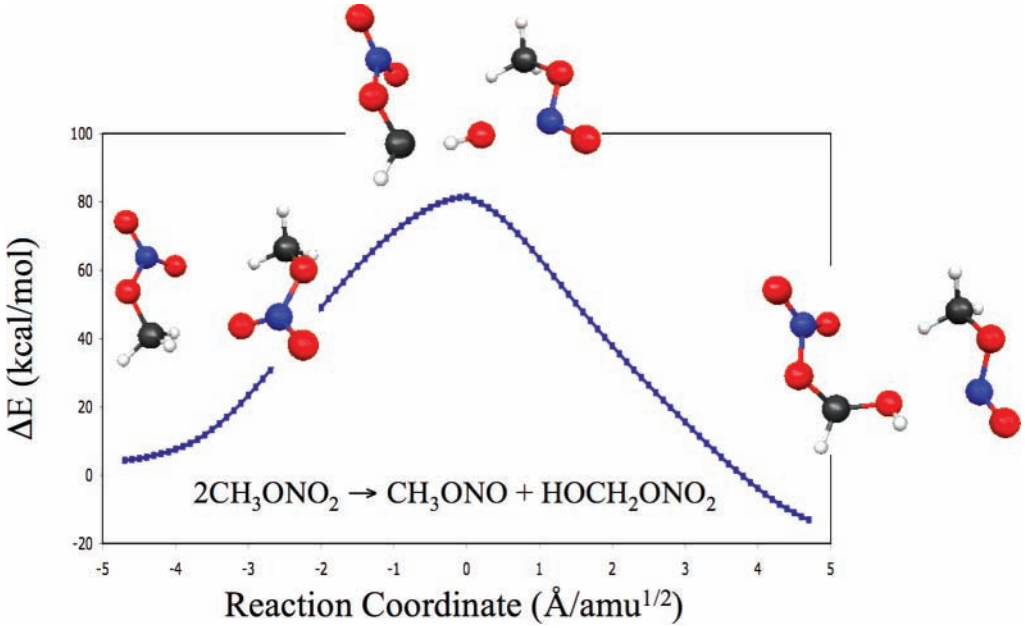

Figure 5. B3-LYP/6-31G* IRC for the bimolecular reaction $2CH_3ONO_2 \rightarrow CH_3ONO + HOCH_2ONO_2$.

SCHEME 2: (a) Mechanism for Reaction of Methylperoxy Radical with Nitric Oxide Including Computed Bond Dissociation Energies in kcal/mol (in parentheses are given the values for the trans conformer). (b) Global Mechanism of Decomposition Reactions of Methyl Nitrate and Methylperoxy Nitrite

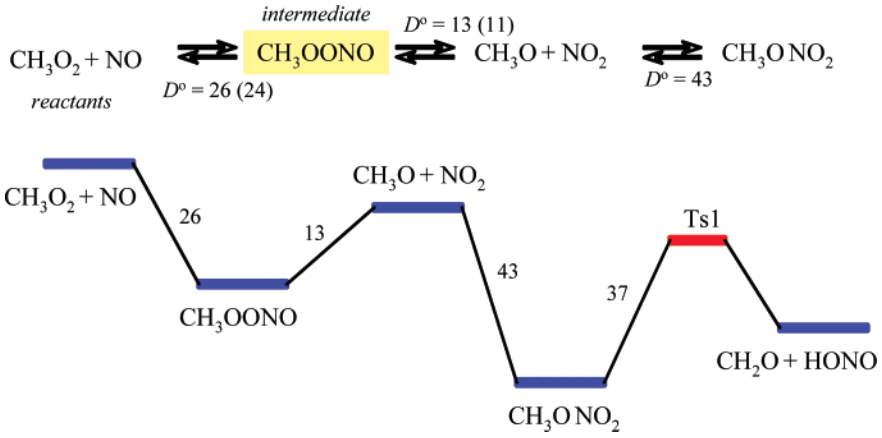

give an incorrect dissociation limit which topologically results on an overestimation of the energy at the dissociation regions of Figure 4b, that is, points (0.; 0.5) and (1.0; 0.5). This fact, in connection with the two minima corresponding to CH_3ONO_2 and CH_3ONO, creates an artificial saddle point. Third, monoconfigurational methods are blind to the S1 state.

For the sake of completeness, we have studied the isomerization of methyl nitrate to *trans*-methylperoxy nitrite and the conclusions that can be extracted there are completely analogous to the cis conformer. The S_0 and S_1 CAS-SCF potential energy surfaces of this process are included in the Supporting Information section (Figure S3).

Formaldehyde Elimination from CH_3ONO_2 and CH_3OONO. Apart from dissociation into radicals, methyl nitrate can react through a parallel channel to yield formaldehyde (CH_2O) and nitrous acid (HONO), $CH_3ONO_2 \rightarrow CH_2O + HONO$. The energy barrier for CH_2O elimination from CH_3ONO_2 amounts to $\Delta U(0) = 37$ kcal/mol at the CASPT2 level, which is 5 kcal/mol lower than that computed for $CH_3ONO_2 \rightarrow CH_3O + NO_2$ (Table 1). The CASPT2 geometry of the transition state (Ts1) for such an elimination is displayed in Figure 1h, and its energetic is collected in Table 1. Compared to CASPT2, density functional theory (B3-LYP) gives similar energetic and geometrical results (Tables S1 and S3). The reason for this has to do with the electronic structure of the transition state, whose dominant configuration corresponds to a closed-shell species. The energy profile of the intrinsic reaction coordinate (B3-LYP) for this reaction is shown in Figure S4.

At the B3-LYP level, elimination of CH_2O from *cis*- or *trans*-methylperoxy nitrite yields in addition nitrous acid (HONO) or isonitrous acid (HNO_2), alternately. In contrast to methyl nitrate, elimination of CH_2O from both conformers of CH_3OONO is energetically less favorable than dissociation into radicals (Table 1 and Table S3). $\Delta U(0)$ for these elimination reactions amounts to 39 and 22 kcal/mol for the cis and trans isomers. Geometrical parameters of the corresponding transition states (Ts5 and Ts6) and IRC calculations starting at them are presented in Table S5 and Figure S5, respectively.

Bimolecular Reaction $2CH_3ONO_2 \rightarrow CH_3ONO + HOCH_2ONO_2$. This reaction was proposed[30] as an alternative possibility to explain the discrepancy between the activation energies reported for the thermolysis (39.8 kcal/mol) of methyl nitrate and the value estimated from thermochemical data (42.1 kcal/mol) for the bond dissociation energy of the $O-NO_2$ bond.

We have studied this reaction at the B3-LYP level. The corresponding transition state (Ts7, Table S6) was found, and the IRC calculation (Figure 5) corroborates that such a transition states certainly connects reactants with products in the above reaction. However, the estimated energy barrier for the process is rather large (73 kcal/mol, Table S2), and therefore this channel must be discarded.

Conclusions

We have studied the chemistry of methyl nitrate and methylperoxy nitrite at the CAS-SCF, CASPT2, and B3-LYP levels of theory. It is found that

(1) There is no minimum energy reaction path for rearrangement of methyl nitrate to CH_3OONO. Although lack of a minimum energy path does not exclude a reaction,[31−33] the barrier that must be surmounted is quite high.

(2) Dissociations of CH_3OONO into radicals ($CH_3O + NO_2$ or $CH_3OO + NO$) are processes without extra exit barriers.

(3) As a consequence of the first and second conclusions, the mechanism given in Scheme 1 must be modified for methyl nitrate according to Scheme 2. That is, nitro−nitrite rearrangement of methyl nitrate to methylperoxy nitrite occurs in a two-step mechanism that implies (i) dissociation into $CH_3O + NO_2$ and (ii) subsequent recombination of the radicals. We attribute the reason for this mechanistic behavior to the existence of an S_1/S_0 conical intersection, which distorts the potential energy surface of the ground state. The proposed mechanism is analogous to that found in the chemistry of nitramide.[22]

(4) The lower energy channel in the decomposition of methyl nitrate is elimination of formaldehyde, $CH_3ONO_2 \rightarrow CH_2O + HONO$. This reaction path is lower indeed than dissociation into radicals, $CH_3ONO_2 \rightarrow CH_3O + NO_2$.

(5) Elimination of formaldehyde from CH_3OONO is energetically less favorable than dissociation into radicals.

To finish, the computed energy barriers and the proposed mechanism (Scheme 2) explain why formaldehyde is only observed at very low pressures (<1 Torr) in the reaction of CH_3O with NO_2.[34−36] That is, the reaction occurs in a two-step mechanism, $CH_3O + NO_2 \rightarrow CH_3ONO_2 \rightarrow CH_2O + HONO$, where the activation energy for the second step is ∼5 kcal/mol lower than that for $CH_3ONO_2 \rightarrow CH_3O + NO_2$. Therefore, if the pressure is not very low, molecular collisions transfer energy from CH_3ONO_2 to a third body and the transition state for $CH_3ONO_2 \rightarrow CH_2O + HONO$ is not yet reachable. Another reaction channel should be the formation of methylperoxy nitrite, $CH_3O + NO_2 \rightarrow CH_3OONO$. However, this intermediate is not observed. The reason has to do with the bond dissociation energy for the reverse process, $CH_3OONO \rightarrow CH_3O + NO_2$, which amounts only to 13 kcal/mol, that is, ∼30 kcal/mol lower than the association of the radicals; as a consequence, collisional energy transfer is not likely to be efficient enough to stabilize this intermediate.

Acknowledgment. This research has been supported by the Spanish Ministerio de Educación y Ciencia (Project BQU2003-1426). The authors thank SCAI (University of Málaga) for economical support to update the MOLCAS 6.2 software package. D.P. thanks the Spanish Ministerio de Educación y Ciencia for the Grant BES-2004-6033, and F.J.A. thanks Junta de Andalucía for the Grant P06-FQM-01895.

Supporting Information Available: CASPT2 tables of energetic and geometrical parameters, intrinsic reaction coordinates, and linear interpolations. This material is available free of charge via the Internet at http://pubs.acs.org.

References and Notes

(1) Atlas, E.; Pollock, W.; Greenberg, J.; Heidt, L. *J. Geophys. Res.* **1993**, *98*, 16933.
(2) Chuck, A. L.; Turner, S. M.; Liss, P. S. *Science* **2002**, *297*, 1151.
(3) (a) Dernall, K. R.; Carter, W. P. L.; Winer, A. M.; Lloyd, A. C.; Pitts, J. N., Jr. *J. Phys. Chem.* **1976**, *80*, 1948. (b) Barker, J. R.; Golden, D. M. *Chem. Rev.* **2003**, *103*, 4577.
(4) Orlando, J. J.; Tyndall, G. S.; Wallington, T. J. *Chem. Rev.* **2003**, *103*, 4657.
(5) (a) Espada, C.; Grossenbacher, J.; Ford, K.; Couch, T.; Shepson, P. B. *Int. J. Chem. Kinet.* **2005**, *37*, 675. (b) Espada, C.; Shepson, P. B. *Int. J. Chem. Kinet.* **2005**, *37*, 686.
(6) Zhang, J.; Dransfield, T.; Donahue, N. M. *J. Phys. Chem. A* **2004**, *108*, 9082.
(7) Atkinson, R.; Aschmann, S. M.; Carter, W. P. L.; Winer, A. M.; Pitts, J. N., Jr. *J. Phys. Chem.* **1982**, *86*, 4563.
(8) Lohr, L. L.; Barker, J. R.; Shroll, R. M. *J. Phys. Chem. A* **2003**, *107*, 7429.
(9) Pan, X. M.; Fu, Z.; Li, Z. S.; Sun, C. C.; Sun, H.; Su, Z. M.; Wang, R. S.; *Chem. Phys. Lett.* **2005**, *409*, 98.
(10) Lesar, A.; Hodoscek, M.; Drougas, E.; Kosmas, A. M. *J. Phys. Chem. A* **2006**, *110*, 7898.
(11) Bacak, A.; Bardwell, M. W.; Raventos, M. T.; Percival, C. J.; Sanchez-Reyna, G.; Shallcross, D. E. *J. Phys. Chem. A* **2004**, *108*, 10681.
(12) Wayne, R. P. In *Chemistry of Atmospheres*, 3rd ed.; Oxford University Press: Oxford, 2000; p 334.
(13) Widmark, P.-O.; Malmqvist, P.-Å.; Roos, B. O. *Theor. Chim. Acta* **1990**, *77*, 291.
(14) Roos, B. O. In *Advances in Chemical Physics: Ab Initio Methods in Quantum Chemistry II*; Lawley, K. P., Ed.; John Wiley & Sons: Chichester, England, 1987; Chapter 69, p 399.
(15) (a) Anderson, K.; Malmqvist, P.-Å.; Roos, B. O.; Sadlej, A. J.; Wolinski, K. *J. Phys. Chem.* **1990**, *94*, 5483. (b) Anderson, K.; Malmqvist, P.-Å.; Roos, B. O. *J. Chem. Phys.* **1992**, *96*, 1218.
(16) Andersson, K., et al. *MOLCAS*, Version 6.2; Lund University: Sweden,
(17) Bearpark, M. J.; Robb, M. A.; Schlegel, H. B. *Chem. Phys. Lett.* **1994**, *223*, 269.
(18) Frisch, M. J., et al. *Gaussian 03*, Revision B.04;
(19) Dunning, T. H., Jr. *J. Chem. Phys.* **1989**, *90*, 1007.
(20) Yarkony, D. R. *J. Chem. Phys.* **1990**, *92*, 2457.
(21) (a) Arenas, J. F.; Otero, J. C.; Peláez, D.; Soto, J. *J. Chem. Phys.* **2005**, *122*, 084324. (b) Arenas, J. F.; Otero, J. C.; Peláez, D.; Soto, J. *J. Phys. Chem. A* **2005**, *109*, 7172. (c) Arenas, J. F.; Otero, J. C.; Peláez, D.; Soto, J. *J. Chem. Phys.* **2003**, *119*, 7814. (d) Arenas, J. F.; Otero, J. C.; Peláez, D.; Soto, J. *J. Org. Chem.* **2006**, *71*, 983. (e) Peláez, D.; Arenas, J. F.; Otero, J. C.; Soto, J. *J. Chem. Phys.* **2006**, 125, 164311. (f) Peláez, D.; Arenas, J. F.; Otero, J. C.; Soto, J. *J. Org. Chem.* **2007**, *72*, 4741.
(22) Soto, J.; Arenas, J. F.; Otero, J. C.; Peláez, D. *J. Phys. Chem. A* **2006**, *110*, 8221.
(23) (a) Becke, A. D. *J. Chem. Phys.* **1993**, *98*, 5648. (b) Lee, C.; Yang, W.; Parr, R. G. *Phys. Rev. B* **1988**, *37*, 785.
(24) (a) Gonzalez, C.; Schlegel, H. B. *J. Chem. Phys.* **1989**, *90*, 2154. (b) Gonzalez, C.; Schlegel, H. B. *J. Phys. Chem.* **1990**, *94*, 5523.
(25) Bode, B. M.; Gordon, M. S. *J. Mol. Graphics Modell.* **1998**, *16*, 133.
(26) Dixon, W. B.; Wilson, E. B., Jr. *J. Chem. Phys.* **1961**, *35*, 191.
(27) Cox, A. P.; Waring, S. *Trans. Faraday Soc.* **1971**, *67*, 3441.
(28) Zhao, Y.; Houk, K. N.; Olson, L. P. *J. Phys. Chem. A* **2004**, *108*, 5864.
(29) (a) Jackels, C. F.; Davidson, E. R. *J. Chem. Phys.* **1976**, *65*, 2941. (b) Jackels, C. F.; Davidson E. R. *J. Chem. Phys.* **1976**, *64*, 2908.
(30) Dewar, M. J. S.; Ritchie, J. P.; Alster, J. *J. Org. Chem.* **1985**, *50*, 1031.
(31) Marcy, T. P.; Díaz, R. R.; Heard, D.; Leone, S. R.; Harding, L. B.; Klippenstein, J. S. *J. Phys. Chem. A* **2001**, *105*, 8361.
(32) Ammal, S. C.; Yamataka, H.; Aida, M.; Dupuis, M. *Science* **2003**, *299*, 1555.
(33) Towsend, D.; Lahankar, S. A.; Lee, S. K.; Chambreau, S. D.; Suits, A. G.; Zhang, X.; Rheinecker, J.; Harding, L. B.; Bowman, J. M. *Science* **2004**, *306*, 1158.
(34) Biggs, P.; Canosa-Mas, C. E.; Fracheboud, J. M.; Parr, A. D.; Shallcross, D. E.; Wayne, R. P.; Caralp, F. *J. Chem. Soc., Faraday Trans.* **1993**, *89*, 4163.
(35) Frost, M. J.; Smith, I. W. M. *J. Chem. Soc., Faraday Trans.* **1990**, *86*, 1751.
(36) Martínez, E.; Albadalejo, J.; Jiménez, E.; Notario, A.; Díaz de Mera, Y. *Chem. Phys. Lett.* **2000**, *329*, 191.